Published in final edited form as:
Nat Struct Mol Biol. 2013 May ; 20(5): 555–565. doi:10.1038/nsmb.2547.

Assembly, analysis and architecture of atypical ubiquitin chains

Manuela K. Hospenthal, **Stefan M.V. Freund**, and **David Komander**[1]
Medical Research Council Laboratory of Molecular Biology, Cambridge, UK.

Abstract

Ubiquitin (Ub) chains regulate many cellular processes, but several chain types including Lys6-linkages have remained unstudied. Here we analyse the bacterial effector E3 ligase NleL (Non-Lee-encoded effector ligase) from enterohaemorrhagic *Escherichia coli* (EHEC) O157:H7, which assembles Lys6- and Lys48-linked Ub polymers. Linkage-specific human deubiquitinases (DUBs) are used to show that NleL generates heterotypic Ub chains, and branched chains are efficiently hydrolysed by DUBs. USP DUBs cleave Lys6-linked polymers exclusively from the distal end, while OTUD3, a DUB with Lys6-preference, can cleave Lys6 polymers at any position within the chain. NleL is utilised to generate large quantities of Lys6-linked polyUb. Crystallographic and NMR spectroscopy analysis reveals that an asymmetric interface between Ile44 and Ile36 hydrophobic patches of neighbouring Ub moieties is propagated in longer Lys6-linked Ub chains. Interactions via the Ile36 patch can displace Leu8 from the Ile44 patch, leading to marked structural perturbations of Ub.

Introduction

Protein ubiquitination is a posttranslational modification that affects many aspects of cellular biology, including the stability of proteins[1], activation of cellular signalling pathways[2], the response to DNA damage[3] and intracellular trafficking[4]. The key to this versatility lies in the ability of ubiquitin (Ub) to form eight structurally and functionally distinct polymers, in which the C-terminus of a distal moiety is attached to one of seven Lys residues (Lys6, Lys11, Lys27, Lys29, Lys33, Lys48 and Lys63) or to the N-terminal Met1 of a proximal moiety[5-7]. The so-formed diubiquitin (diUb) can be extended in homotypic Ub chains, where all linkages are of the same chain type, or in heterotypic Ub chains that comprise alternating linkage types or branches[5-7]. Differently linked Ub chains mediate distinct cellular responses. While Lys48- and Lys11-linked polyUb act as proteasomal degradation signals[8,9], Lys63- and Met1-linked Ub chains have various non-proteolytic roles[2,10]. Little is known about the remaining linkage types.

[1]Corresponding author: dk@mrc-lmb.cam.ac.uk.

Accession numbers Coordinates and structure factors for Lys6 triUb have been deposited with the protein data bank, entry 3zlz.

Author Contributions MKH and DK designed, and MKH performed and analysed all experiments in this manuscript, with help from SMVF for NMR analysis. DK wrote the manuscript with help from all authors.

Competing Financial Interests DK is a consultant for Mission Therapeutics.

Europe PMC Funders Author Manuscripts

Lys6-linkages are readily detected in yeast[11] and in mammalian cells[12-14]. This Ub chain type has been indirectly linked to DNA repair processes since the BRCA1/BARD1 Ub ligase complex was reported to assemble polyUb with Lys6-linkages on itself[15-17] and on substrates[16,18-20]. The related Ring1B/Bmi1 polycomb E3 ligase complex assembles heterotypic Ub chains with branches at Lys6, Lys27 and Lys48 *in vitro*[21]. However the cellular roles of Lys6-linkages are currently unclear, but may not be linked to proteasomal degradation, as its levels do not increase with proteasome inhibition[13,14] and as it does not seem to destabilise its substrates[16,18-20]. Lys6-linked diUb (Lys6 diUb) has been produced using chemical biology protocols[22,23], and preliminary structural insights into this Ub chain type suggest a compact conformation[23]. Large-scale enzymatic synthesis of Lys6-linkages has not been achieved, and linkage-specific Ub binding domains (UBDs[24]) or deubiquitinases (DUBs[25,26]) for this chain type are currently unknown.

Recently, a bacterial Ub E3 ligase related to HECT family enzymes was shown to assemble Lys6- and Lys48-linked Ub chains *in vitro*[27]. The protein NleL (Non-Lee-encoded effector ligase) from enterohaemorrhagic *Escherichia coli* (EHEC) O157:H7 is a bacterial effector protein that is injected into host cells by a type III secretion system (TTSS)[28]. NleL activity restricts the formation of actin-rich pedestals that form beneath the adherent bacterium on the host cell surface. It was shown that NleL activity limits the number of pedestals, and the catalytic activity of the *Citrobacter rodentium* NleL homolog is required for efficient infection of colonic epithelial cells in mice[28].

Here we exploit NleL to generate large quantities of Lys6 polyUb enabling detailed biochemical and structural analysis of this atypical Ub chain type. NleL is capable of forming heterotypic Ub chains *in vitro* and we show that it can use both Lys6 and Lys48 for Ub chain extension. We use linkage-specific DUBs to evaluate the architecture of heterotypic Ub chains. Solution studies on Lys6-linkages reveal an asymmetric interface in Lys6 polymers, in which hydrophobic Ile44 and Ile36 patches of Ub interact to form a compact structure that also features a conformational change in Ub itself.

Results

NleL assembles heterotypic Lys6 and Lys48 Ub linkages *in vitro*

We produced NleL in bacteria, and characterised its *in vitro* chain assembly capability using E1 and UBE2L3/UbcH7. NleL assembled unanchored Ub chains with wild type (WT) Ub, and the set of single-lysine Ub mutants showed NleL specificity for Lys6 and Lys48 (Fig. 1a), as reported previously[27]. Mutation of either Ub Lys6 or Lys48 to Arg (K6R or K48R) resulted in free Ub chains of the other type, while a double mutant K6R K48R was unable to assemble unanchored Ub chains efficiently (Fig. 1b).

Electrophoretic mobility of Ub chains with three or more Ub molecules varies with linkage type, which can be used diagnostically[29]. We observed a double band for diUb assembled from WT Ub, indicating different electrophoretic mobility of Lys6 and Lys48 diUb. In longer chains (e.g. pentaUb, Fig. 1b, c) the electrophoretic mobility of WT polymers is different to that of both Ub point mutants, suggesting that NleL assembles heterotypic Ub chains comprising both Lys6- and Lys48-linkages in the same polymer (Fig. 1b, c).

Comparison of the assembly of Ub K6R with Ub K48R into homotypic Ub chains over a short time course shows that the kinetics of assembly of diUb with Lys48- or Lys6-linked chains is similar (Fig. 1c). Interestingly, while Lys6-linkages were assembled into long polymers within minutes, assembly of Lys48-linkages appeared to progress with slower kinetics, generating diUb and small amounts of triUb under identical conditions (Fig. 1c).

Using linkage specific DUBs to study chain topology

The question regarding the topology of NleL-assembled polyUb remained, and the amount and length of Lys6 vs. Lys48 chains in NleL conjugates with WT Ub was unclear. The architecture of heterotypic Ub chains is difficult to assess by current technologies such as mass-spectrometry[30].

We hence set out to establish biochemical approaches to assess Ub chain architecture. Even at short chain length and with only two linkage types, the combinatorial complexity of heterotypic Ub chains is immense. The number of species in a Ub chain with *n* Ub molecules comprising two linkage types can be calculated using Catalan numbers[31] (see **Methods**). For tetraUb, 14 different species can be produced (Fig. 2a).

We used linkage-specific DUBs as ‘Ub chain restriction enzymes’ in ‘Ub chain restriction analysis’, to reveal building blocks comprising distinct linkages as well as the predominant linkage type of the assembly reaction (Fig. 2a).

Human ovarian tumour (OTU) DUBs are ideal for this purpose as many members display marked linkage preference[32,33]. The Lys48-specific enzyme OTUB1[34] was unable to cleave Lys6 di- or tetraUb under conditions where Lys48 chains were quantitatively hydrolysed (Fig. 2b). A DUB that preferred Lys6- to Lys48-linkages has not been reported. When we tested human OTU domain DUBs for activity against differently linked diUb species (Tycho E.T. Mevissen, MKH and DK, unpublished data), we discovered that the uncharacterised DUB OTUD3 showed strong activity against Lys6-linkages, but was significantly less active against Lys48 chains (Fig. 2c). The non-specific viral OTU domain (vOTU) from Crimean Congo Haemorrhagic Fever Virus[35] hydrolysed Lys6- and Lys48-linkages similarly (Supplementary Fig. 1a).

Together, vOTU, OTUB1 and OTUD3 were used to analyse Ub chain architecture of NleL assembled WT Ub chains *in vitro*. vOTU, or a combination of OTUB1 with OTUD3 hydrolysed purified heterotypic penta/hexaUb quantitatively, revealing that DUBs can access all linkages in the heterotypic polymers (Fig. 2d, lanes 11-16). Interestingly, OTUB1 alone disassembled heterotypic Ub chains to mono-, di-, tri-, and tetraUb (Fig. 2d, lanes 5-7). OTUD3 treatment resulted in a different banding pattern, with mainly mono- and diUb and a faint signal for triUb (Fig. 2d, lanes 8-10). The resulting Ub chains are different as they show distinct electrophoretic mobility (Fig. 2d, compare lanes 6 and 9, and Fig. 1b), and can be identified as Lys6- or Lys48-linked due to their running behaviour on SDS-PAGE gels (see below).

The results from Ub chain restriction analysis hence reveal that NleL-assembled free Ub chains comprise both Lys6- and Lys48-linkages. Lys6-linkages seem to predominate and are

found in longer stretches, yet most individual polymers also seem to comprise at least one Lys48-linkage.

We next tested whether NleL assembles heterotypic Ub chains on substrates. UBE2L3 was strongly polyubiquitinated *in vitro*, in an NleL-dependent manner (Fig. 2e), and a Lys-less E2 mutant in which the 18 Lys residues were changed to Arg (UBE2L3 noK), still promoted assembly of free Ub chains, but remained unmodified (Fig. 2e). Polyubiquitinated GST-UBE2L3 was immobilised with GSH resin, and treated with different DUBs as before (Fig. 2f). While vOTU completely removed polyUb from UBE2L3, some polyUb remained after OTUB1 and OTUD3 treatment. Interestingly, as in the reaction on free chains, OTUD3 released small amounts of presumably Lys48-linked diUb (Fig. 2f). Western blotting for UBE2L3 revealed that both OTUB1 and OTUD3 generated a similar pattern of, presumably, multi-monoubiquitinated GST-UBE2L3, and indicated that vOTU removed at least some of this monoUb from the protein.

NleL can assemble branched Ub polymers

Ub chain restriction mapping unambiguously revealed heterotypic Ub chains, but could not distinguish whether such Ub chains featured mixed or branched linkages. To test whether NleL can assemble branched species in which one acceptor Ub is modified at both Lys6 and Lys48 simultaneously, an assembly reaction was performed with Ub ΔG76 as the acceptor, and Ub K6R K48R as the donor Ub (Fig. 3a). Indeed, NleL assembled branched triUb efficiently (Fig. 3b, c), showing that NleL has the propensity to assemble branched chains indicating that all NleL products depicted in Fig. 2a potentially exist.

In addition to the branched triUb, a higher molecular weight band also appeared in the reaction, and western blotting showed that this band contained Ub. This band was still present when a Lys-less UBE2L3 mutant was used, suggesting that it was not a modified form of the E2 enzyme (Fig. 3d). NleL could assemble low amounts of Lys11-linked diUb when none of the preferred Lys residues were available (e.g. in a Lys11 only mutant Ub, Fig. 1a). Treatment with the Lys11-specific OTU DUB Cezanne[32] depleted the tetraUb species, revealing that this species indeed contained a Lys11-linkage. Cezanne did not reduce the amounts of branched triUb or diUb significantly.

Hydrolysis of homotypic and heterotypic Ub chains by DUBs

We next characterised whether and how DUBs hydrolyse branched and Lys6-linked polyUb. Purified branched triUb was treated as before (Fig. 2d). OTUD3 and OTUB1 hydrolysed their preferred linkages identically regardless of whether the Ub chain was homotypic or branched (Fig. 4a). Similar results were obtained with vOTU and with DUBs from the USP family (USP7, USP21) (Fig. 4b-d). It hence seemed that chain topology in this simple case does not pose a problem for the analysed enzymes. A limitation of this assay is the low complexity of the Ub polymer and the fact that the chains are not attached to a substrate.

Indeed, we suspected that different families of DUBs would hydrolyse Lys6-linked polyUb differently, due to the different structures and binding interfaces in the catalytic domain. All DUB families bind to a distal Ub via a high-affinity S1 Ub binding site that depending on

the DUB family covers between 20% and 40% of the Ub surface[25]. In small OTU domains such as OTUD3 or *S. cerevisiae* Otu1, the Lys6 side chain of the bound Ub is solvent exposed and accessible (Fig. 4e). In contrast, USP domain enzymes such as USP21 contact Lys6 and neighbouring residues in their Ub binding site (Fig. 4f). This difference in binding mode has consequences for how Lys6-linkages are hydrolysed by these enzymes. OTUD3 could bind and hydrolyse any Ub-linakge in a Lys6-linked polymer, showing *endo*-activity. This can be appreciated in a short time course of pentaUb cleavage by OTUD3, in which even at early timepoints, all possible products (monoUb, diUb, triUb, tetraUb) are produced (Fig. 4g). In contrast, USP21 cannot bind to internal Ub moieties (in which Lys6 would be modified), but must interact with the distal tip of the chain. USP21 cleavage accordingly resulted in a stepwise hydrolysis of Lys6-linked chains, with monoUb as a main product, and generation of diUb at later timepoints when triUb had first been produced (Fig. 4h). It is interesting to note that OTU and USP enzymes cleave other chain types, e.g. Lys63-linked polyUb, with *endo*-activity[29,36]. Hence, the mechanism by which DUBs cleave polyUb depends both on the DUB family and on the Ub linkage within the chain.

Large scale assembly and crystal structures of Lys6 polyUb

We utilised NleL to perform large-scale enzymatic synthesis of Lys6 polymers for further analysis. A protocol was devised in which 25 mg of Ub K48R was assembled into unanchored Ub chains of varying lengths that were subsequently separated using size-exclusion chromatography (SEC) (see **Methods**, Fig. 5a-c). This allowed access to homogeneous Lys6 di-, tri- and tetraUb in which each moiety comprises a K48R mutation.

The remarkable specificity of OTUB1 also enabled large-scale generation of WT Lys6-linked chains. For this, heterotypic Ub chains were assembled from 25 mg WT Ub, and the reaction was subsequently treated with OTUB1, which cleaved all Lys48-linkages within the polymers. Subsequent purification of the products generated milligram quantities of WT Lys6 chains (Fig. 5d)

Access to milligram quantities of Lys6 polymers allowed detailed structural analysis of this atypical Ub chain type. Crystals of Lys6 triUb diffracted to 3.0 Å, and of Lys6 tetraUb to 3.8 Å resolution (Table 1, Fig. 5e, Supplementary Fig. 2). However, these crystals formed with identical space group ($P4_32$) and unit cell dimensions as we had previously observed for Lys6 diUb[23]. Moreover, Lys63- and Met1-linked diUb[29] and monoUb[37] crystal structures have been obtained from this crystal form. Since the asymmetric unit contains only two Ub molecules, Lys6 tri- and tetraUb crystallised over neighbouring asymmetric units, forming one ‘tight’ interface between Ub molecules in the same asymmetric unit, and one ‘loose’ interface between Ub molecules from neighbouring asymmetric units (Fig. 5e). The isopeptide linkages between molecules are not resolved (Fig. 5e). Hence, a crystalline low energy state of many Ub polymers is described in a single high-symmetry crystal form, suggesting that strong lattice forces may compete with weak intra-chain Ub interactions. The low resolution observed in Lys6 polymers (3.0-3.8 Å[23]) further suggests strains on the packing not observed with high resolution Lys63 or Met1 diUb (1.9 and 2.2 Å[29]).

Nevertheless, the conformation observed in the Lys6 polyUb structures is appealing and deserves further consideration. A hydrophobic interface is formed between Ub moieties,

using the common Ile44 hydrophobic patch (residues Ile44, Leu8, Val70, His68) on the proximal Ub, and a less common, orthogonal hydrophobic interface centred around Ile36 (residues Ile36, Leu71, Leu73) on the distal Ub[23]. Notably, the distal Ub shows a marked conformational change, whereby Leu8 in the flexible β1/β2-loop no longer participates in the Ile44 but rather in the Ile36 patch[23]. To test whether this novel conformation of polyUb also forms in solution, we turned to nuclear magnetic resonance (NMR) spectroscopy.

Solution studies of Lys6 diUb

NMR spectroscopy is ideal to study dynamic Ub chains and has been used extensively to study Ub chain conformation[32,38,39]. We first analysed ^{15}N-labelled Lys6 diUb (containing K48R mutations) (Fig. 6a, see **Methods**). ^{1}H, ^{15}N-heteronuclear single-quantum correlation (^{1}H, ^{15}N-HSQC) spectra were compared to a ^{15}N-labelled Ub K48R reference spectrum. While most resonances were unperturbed (Fig. 6b, resonance Gln2), the observed doubling of a subset of resonances in the Lys6 diUb spectrum indicates that an interface between the two Ub moieties is formed. Two phenomena can be distinguished. We observed a new peak position in addition to a peak position matching the reference spectrum. Such residues are part of the interface in one of the two Ub moieties, indicating that an asymmetric interface is formed (Fig. 6b, resonance His68). Alternatively, for a small number of residues we observed two new peak positions relative to the reference, suggesting that these residues are involved in the interface on both the proximal and distal moieties of Lys6 diUb (Fig. 6b, resonance Leu8).

To understand the contribution of each Ub moiety to the interface, species of Lys6 diUb were assembled in which either the proximal or the distal moiety was ^{13}C, ^{15}N-labelled (see **Methods**, Fig. 6a). Reassigned ^{1}H, ^{15}N-HSQC spectra of proximally and distally labelled Lys6 diUb enabled the unambiguous distinction between distal and proximal resonances in the uniformly ^{15}N-labelled Lys6 diUb spectrum (Fig. 6b). Chemical shift perturbation (CSP) maps covering either the proximal or the distal moiety are shown in Fig. 6c and 6d.

Significant CSPs (Δppm > 0.035) were mapped onto the surface of Ub. On the proximal Ub (Fig. 6e), the largest CSPs are found in regions surrounding residues 5-8 (including Lys6), 42-50, and 68-74. Proximal CSPs map to a contiguous surface on Ub that corresponds to the Ile44 hydrophobic patch (Fig. 6e). The only residue that does not show significant perturbations within this surface is Val70 (Fig. 6c, e).

The picture is less clear on the distal moiety where fewer resonances are significantly perturbed (Fig. 6d, f), generating a disconnected patch when mapped onto the Ub surface (Fig. 6f). In agreement with Ile36 interaction, Gly35, Ile36 and Leu73 are perturbed, yet Glu34, Gln40 and Leu71 located nearby do not experience significant perturbation (Fig. 6f). In contrast, a second remote surface patch comprising Thr12, Ile13 and Thr14 on the β2-strand of Ub show strong CSPs (Fig. 6d, Supplementary Fig. 3a). These three residues however do not form an interaction surface comparable to that observed on the proximal interface (Fig. 6e, f) (see below). We excluded that this is an effect of ring current caused by the nearby Phe4 side chain, by mutating this residue to Leu (Ub F4L) and conducting further NMR experiments (Supplementary Fig. 3b, c).

Overall, the solution interface of Lys6 diUb confirms that this Ub chain type is compact, forming a clear proximal Ile44 patch interaction with the distal unit. The residues perturbed in the distal interface are consistent with an Ile36 patch interaction, however this interface is less well defined. Interestingly this was observed previously in Lys48 diUb, which interacts *via* Ile44 interfaces on both moieties, yet the proximal interface was significantly better defined compared to the distal interface[40]. This may reflect a more dynamic interaction surface rather than a rigid binding site.

Solution studies of Lys6 triUb

Importantly, the Ile44 patch region (residues 42-50) on the distal moiety is unperturbed and this patch may be available for Ub chain propagation. A structural model for Lys6 triUb based on propagating the 'tight' interface seen in the crystal structure (Fig. 5e) does not result in steric clashes, yet some additional interactions would be predicted between the first and the third moiety in the Ub chain (Fig. 7a).

We reasoned that if the interfaces were propagated, we would observe similar CSPs in longer Lys6 polyUb compared to diUb. We hence assembled Lys6 triUb species in which either the distal or the proximal Ub was ^{13}C, ^{15}N-labelled (Fig. 7b, c, see **Methods**). ^{1}H, ^{15}N-HSQC spectra of these species were compared to Lys6 diUb, and CSP maps generated (Fig. 7b, c).

As can be appreciated in Fig. 7b and 7c, the spectra of distally or proximally labelled Lys6 tri- and diUb are virtually identical with only small variations in CSPs. The only residues that are perturbed are Leu71 and Leu73 in the distally labelled sample, suggesting that this region might be involved in additional interactions in longer Lys6 chains, which is consistent with the predicted model (Fig. 7a).

We next labelled the middle Ub in triUb, to achieve a species that interacts via both Ile36 and Ile44 patches with neighbouring moieties (Fig. 7d). The resulting spectra revealed an unanticipated complex scenario, in which many resonances showed strong CSPs, and experienced splitting. Nevertheless, mapping of all perturbed resonances onto the surface of Ub showed that indeed, the main perturbations are in the Ile36 patch and the Ile44 patch, consistent with the structural models (Fig. 7e). This is consistent with chain propagation via the observed asymmetric interfaces in longer Lys6 polyUb (Fig. 7f).

However, the complex spectrum of the middle-labelled triUb suggested the presence of additional effects. Resonances in the Ile36 patch (Ile36, Leu73) were perturbed as previously observed in the distally labelled diUb spectrum (Fig. 7g, Supplementary Fig. 4), indicating perturbations due to interface formation. In contrast, resonances in the flexible β1/β2-loop of Ub were split, indicating that the middle moiety in this triUb is exchanging between two conformations. Resonance splitting was observed also for the Thr12-Ile13-Thr14 region, which was perturbed when the Ile36 patch is engaged in the distally labelled diUb (Fig. 6d). Strangely, the Ile44 patch also shows resonance splitting in this species. Together, this suggests that in context of neighbouring units in Lys6-polyUb, Ub itself undergoes significant conformational changes and exists in multiple conformations.

NMR analysis of an Ile36 patch-interacting UBD

Experiments on the middle-labelled triUb, and the lingering issue of large CSPs in residues Thr12, Ile13 and Thr14 of the distal moiety (see above, Fig. 6d), prompted us to analyse whether this was due to engagement of the Ile36 patch. To investigate this, we characterised monoUb binding to the zinc finger Ub binding domain of USP5/IsoT (ZnF UBP), which is the only known UBD to date that binds the Ile36 surface exclusively[41] (Fig. 8a, b). Interactions with the C-terminus of Ub and the Ile36 patch are mediated by an extended hydrophobic loop that contacts Ile36, Leu71, Leu73, and also Leu8, the latter being in a conformation as observed in the distal Ub of Lys6 diUb (see below). The Ile44 patch and residues 12-14 of Ub are solvent exposed[41] (Fig. 8b).

NMR studies using ^{13}C, ^{15}N-labelled WT Ub and unlabelled ZnF UBP, revealed that ZnF UBP significantly perturbed the Ub structure, resulting in large CSPs and exchange broadening in several resonances, requiring titration of ZnF UBP to reconcile assignments of Ub resonances (Fig. 8c-f). This is in accordance with the high binding affinity previously reported for this interaction (2.8 μM, [41]). Leu8 is completely exchange broadened upon addition of ZnF UBP indicating that this residue is important in the interaction (Fig. 8d, e). Thr9 is exchange broadened in monoUb but reappears when Ub is in complex with ZnF UBP, also indicating a dynamic change of the β1/β2-loop region (Fig. 8e). Mapping of perturbed and exchange broadened residues onto the surface of Ub (Fig. 8f) resulted in a near-perfect match with the crystallographic interface (Fig. 8b). The CSPs caused by high affinity binding of ZnF UBP are similar to those seen in the distal Lys6 diUb spectrum (Fig. 4, Supplementary Fig. 5).

Importantly, residues 12-14 are perturbed significantly by ZnF UBP (Fig. 8c-e), and also resonances on other β-strands not involved in ZnF UBP interactions experience perturbation, most notably residues in the Ub Ile44 patch (e.g. Ile44, His68, Leu69, Val70). This partly explains perturbation of resonances in the middle-labelled Lys6 triUb species, in which the Ile36 interface was engaged, and the β-strands were perturbed despite not being directly engaged by intra-chain polyUb contacts.

Ile36 patch interactions perturb Ub structure

The simplest explanation for these observed perturbations is that Ile36 interactions perturb Ub structure. The most flexible region in Ub is the Ub β1/β2-loop which spans residues 6 to 12 (ref. [42]). In most structures of monoUb determined to date and also in the proximal Ub in Lys6 diUb, Leu8 at the tip of this loop contributes to the Ile44 hydrophobic patch, and the β1/β2-loop is flipped outwards (‘loop-out’ position) (Fig. 9a). As mentioned above, in the distal Ub of Lys6 diUb and in the ZnF UBP complex, Leu8 contributes to the Ile36 patch, due to a marked conformational change of the β1/β2-loop which is now more closely attached to the Ub core (‘loop-in’ position) (Fig. 9b)[23].

Overlaying crystal structures of the different conformations revealed significant reorientation of the β1/β2 strands, likely accounting for the observed strong CSPs. In addition, a large RDC ensemble of monoUb[42] (Fig. 9c, d) contains both Leu8 conformations, and different loop-conformations correlate with changes in Ub core

structure. In the ‘loop-out’ position, the β2-strand nudges more tightly towards the Ub core allowing Ile13 to form stronger hydrophobic contacts with residues such as Ile30. Conversely, in the ‘loop-in’ position, the whole molecule relaxes slightly, and e.g. the Ile44 position is more flexible (Fig. 9d). These long-range correlated motions in Ub have been reported previously[43]. The fact that some of the observed Ub perturbations originate from conformational changes within one Ub rather than from interface formation between linked Ub molecules, highlights that CSPs should be interpreted with caution, as they do not necessarily always reflect interface formation.

Our results indicate that Ile36 patch interaction can lead to a conformational switch involving the β1/β2-loop, resulting in global rearrangements within Ub. To examine whether this was a common phenomenon, we analysed crystal structures of Ub complexes that involved the Ile36 patch (Fig. 9f). In many but not all cases, Ile36-binding stabilised the ‘loop-in’ conformation of Ub. Examples include the discussed Lys6 diUb, ZnF UBP and also the CUE domain of Vps9p[44] that interacts with both Ile36 and Ile44 patches simultaneously (Fig. 9f). Interestingly the ‘loop-in’ conformation of Ub is also observed in recent crystal structures of RING E3 ligases bound to a charged E2 enzyme[45,46], in which the E2 interacts with the Ile44 and the RING interacts with the Ile36 patch on Ub (Fig. 9f). Examples where the Ile36 patch is engaged, but Ub is in a loop-out position are found in the crystal structures of Lys11-linked diUb[32,47], and in HECT domain E3s that bind the Ub Ile36 patch via the N-lobe[48,49], and via the C-lobe[50] (Fig. 9f). This shows that Ile36 patch interactors stabilise different Ub conformations whilst binding this hydrophobic surface. The fact that RING E3 ligases use the Ile36 surface and exploit the flexibility of the β1/β2-loop suggests that both features are of functional importance.

Discussion

We here describe an enzymatic assembly system for Lys6-linked polyUb chains. The enzyme used for the assembly reaction, NleL, originates from the bacterial human pathogen EHEC O157:H7, one of many pathogens affecting ubiquitination[51,52]. NleL is involved in infectivity although its cellular targets are unknown[28]. The observation that NleL assembles a previously undescribed linkage combination suggests that EHEC O157:H7 interferes with the Ub system in novel ways. It is unclear what advantage this pathogen gains by mixing these linkage types, but it is interesting to see that pathogens exploit the full combinatorial potential of the Ub system.

To characterise the complexity of chain products generated by NleL, we introduce Ub chain restriction analysis, in which linkage specific DUBs are used to investigate which chain types are present on a substrate, and to characterise polyUb architecture. This showed that (i) NleL assembles free and substrate-attached heterotypic Ub chains in which (ii) most individual polymers comprise more than one linkage type. Furthermore, NleL-assembled Ub chains are (iii) predominantly Lys6-linked and (iv) comprise rarely more than one or two Lys48-linkages in series. We believe linkage-specific DUBs will have many applications in the future, in particular to answer open questions regarding chain architecture.

Few reports have addressed the vast combinatorial potential in branched Ub chain structures, and their abundance and relevance is unclear. It is known that many RING E3 ligases generate branched Ub chains *in vitro* when used with non-specific E2 enzymes such as UBE2D/UbcH5, and complex branched polymers were shown to be non-degradable[53]. We found simple branches (in a branched triUb) do not pose problems for non-specific USP and OTU enzymes or for specific OTU DUBs. Hence, in addition to Ub binding proteins that can prevent the formation of branched polymers[54], also (linkage-specific) DUBs could serve to prevent the emergence of potentially toxic branched polymers generated by non-specific ligase systems.

Structurally, Lys6 chains adopt compact conformations comprising an asymmetric hydrophobic interface between neighbouring Ub moieties. The interface is propagated in longer Ub chains, resulting in a compact conformation for Lys6 polymers distinct from known Ub chain structures. In such a polymer structure, the Ile44 and Ile36 patches would be shielded from solvent in internal Ub moieties. This unique chain structure may attract novel Ub binding domains and proteins, which need to be identified in future work.

Our observation of an Ile36-based interface prompted a more detailed characterisation of this emerging Ub binding interface, that was recently shown to be important for E3 ligase interactions with Ub[45,46,50]. This highlights that the known conformational plasticity in Ub[42] is exploited by UBDs, E3 ligases, and also in polyUb interactions. Mutations of Ile44, Val70 or Leu8 prevent vegetative growth of *S. cerevisiae*[55], highlighting the importance of the common Ile44 Ub binding site in Ub biology. Interestingly, mutation of Ile36, Leu71 and Leu73 also inhibit yeast growth[55], suggesting similar functional importance for the Ile36 patch, and we anticipate that more UBD classes recognising this Ub surface exist.

Online Experimental Procedures

Constructs

A vector encoding GST-NleL 170-782 was a kind gift from David Yin-Wei Lin and Jue Chen[27]. Constructs for E1[59], UBE2L3/UbcH7[60], OTUB1[61], vOTU[35], USP5 ZnF UBP[41], USP21[36], USP7[62] have been described previously. The catalytic domain of human OTUD3 (residues 52-209) was cloned into the pOPIN-K vector[63]. Ub mutants encoded on the pET17b vector were generated by site-directed mutagenesis according to the QuikChange protocol but using KOD polymerase (Merck Chemicals). DNA for a Lys-less mutant of UBE2L3 (noK UBE2L3) where all 18 Lys residues are replaced by Arg was synthesised (Genscript) and cloned into the pOPIN-K vector[63].

Protein production

Recombinant GST-fusion proteins (OTUD3, ZnF UBP, UBE2L3 variants) were expressed in Rosetta2 (DE3) pLacI cells (Novagen). Cultures were grown in LB media to OD_{600} of 0.6-0.8 and induced using 0.1-1.0 mM IPTG at 20°C for 12 h. Cells were lysed by sonication and proteins were purified using Glutathione Sepharose 4B (GE Healthcare) followed by incubation of beads with PreScission protease to remove the GST-tag. Eluted proteins were further purified by anion exchange chromatography (RESOURCE Q, GE

Healthcare) and size-exclusion chromatography (SEC) (Superdex 75, GE Healthcare) in SEC buffer (50 mM Tris [pH 8.5], 150 mM NaCl, 5 mM DTT) or NMR buffer (18 mM Na_2HPO_4, 7 mM $NaH_2PO_4 \times 2H_2O$ [pH 7.2], 150 mM NaCl). All purifications were performed at 4°C. Proteins were concentrated using Amicon spin concentrators (3 kDa MW cut-off). NleL was purified according to[27], OTUB1 according to[61], vOTU according to[35], USP7 according to[62], USP21 according to[36], E1 according to[59] and Ub mutants according to[64].

In vitro ubiquitination assays

Small-scale analytical ubiquitination assays were carried out in 20 μL reactions by incubating 57 μM Ub or Ub Lys-only mutants, 125 nM Ub activating enzyme (E1), 2.24 μM UBE2L3/UbcH7 Ub conjugating enzyme (E2), 1.56 μM NleL Ub ligase (E3), 10 mM ATP, 40 mM Tris (pH 7.5), 10 mM $MgCl_2$, 0.6 mM DTT, at 37°C for 30 min. The reaction was stopped by the addition of 10 μL 4 × LDS sample buffer (Invitrogen) and samples were analysed by SDS-PAGE, using 4-12% NuPAGE gradient gels with MES buffer (Invitrogen) and coomassie stained using Simply Blue Safe Stain (Expedeon protein solutions). Alternatively, samples were analysed by Western blotting using a 1:2000 dilution of anti-Ub (rabbit polyclonal from Millipore) or a 1:3000 dilution of anti-UBE2L3 (rabbit polyclonal against aa 111-125, Sigma) antibody and bands were visualised by enhanced chemiluminescence (ECL Prime, Roche).

Large-scale Lys6 chain assembly

Large-scale assembly of Lys6 polymers from Ub K48R was carried out in 1 mL reactions from 25 mg Ub K48R (2.91 mM), 0.1 μM E1, 0.56 μM UBE2L3/UbcH7, 11.1 μM NleL, 10 mM ATP, 40 mM Tris (pH 7.5), 10 mM $MgCl_2$, 0.6 mM DTT, at 37°C for 3-4 h. Subsequently, 5 μL of 4 M HCl was slowly added to the reaction, which reduces the pH to 4.0-5.0 and precipitates enzymes. The reaction was centrifuged (16000 × *g*, 4°C), filtered and purified by SEC (Superdex 75, GE Healthcare) in 50 mM Tris (pH 7.6). Peak fractions containing Lys6 di-, tri- and tetraUb were pooled and concentrated.

To generate WT Lys6 polyUb, an assembly reaction was performed as above with 25 mg WT Ub, and after 3 h, 5 μM OTUB1 was added to the reaction, and further incubated overnight. Chains were purified as for Ub K48R.

In vitro deubiquitination assays and Ub chain restriction mapping

In vitro DUB assays were performed as described previously[29]. PolyUb (2-4 μg) was incubated at 37°C with 4.7 μM OTUB1, 5.5 μM OTUD3 or 6.1 nM vOTU in 40 μL reactions. At each timepoint, 5 μL of the reaction was stopped by mixing with 5 μL of 4 × LDS sample buffer and analysed by SDS-PAGE. Protein was visualised by silver staining using the Silver Stain Plus Kit (Bio-Rad) following the manufacturer's protocol. For Ub chain restriction analysis of UBE2L3, a GST-tagged construct of UbE2L3 was used in ubiquitination assays as described above. The E2 enzyme was subsequently immobilised on Glutathione Sepharose 4B (GE Healthcare) and incubated with DUBs at the above concentrations for 1 h at 37°C in 20 μL reactions. Reactions were analysed by Western blotting as described above.

Generation of labelled Ub chains for NMR analysis

Ub mutants were expressed in Rosetta 2 (DE3) pLacI cells, in minimal media (M9 minus - lacking NH_4Cl) which was supplemented with 2 mM $MgSO_4$, 50 μM $ZnCl_2$, 10 μM $CaCl_2$, trace elements, antibiotics, 2 g $^{15}NH_4Cl$ and 4 g glucose ($^{13}C_6$ glucose for doubly labelled proteins). Protein expression was induced at an OD_{600} of 0.6-0.8 with 1 mM IPTG, and cells were harvested after 4 h growth at 37°C. Labelled Ub mutants were purified as described previously[65]. Lys6 chains were assembled from selected Ub mutants as detailed in Supplementary Table 1, in a large-scale assembly reaction using NleL as described above. The Lys6-linked middle ^{13}C, ^{15}N-labelled triUb was assembled using NleL in large-scale assembly reactions (see above) in two steps. First, diUb was assembled using a 1:1 molar ratio of ^{13}C, ^{15}N-labelled Ub K48R and unlabelled Ub K48R harbouring a non-cleavable C-terminal His6-tag. In addition, this construct lacked Gly76 to prevent proteolysis of the His6-tag during expression in Rosetta 2 (DE3) pLacI cells. The correct diUb product was purified by Ni-NTA immobilised metal affinity chromatography (IMAC) and used subsequently in the second reaction together with an unlabelled donor Ub K48R K6R in a 1:1 molar ratio. Middle ^{13}C, ^{15}N-labelled Lys6-linked triUb was then purified by SEC in NMR buffer and concentrated to 37 μM.

All other Lys6 di- and triUb species were also purified by SEC with NMR buffer and used in NMR experiments. These samples were concentrated to final concentrations of 80-100 μM.

USP5 ZnF UBP was purified by SEC in NMR buffer including 5 mM DTT for all NMR binding experiments involving this UBD (Fig. 7, 8). Proteins were concentrated and protein concentration was assessed using BCA assays (Thermo Scientific).

NMR spectroscopy

NMR acquisition was carried out at 298 K on Bruker Avance III 600 MHz and Avance2+ 700 MHz spectrometers equipped with cryogenic triple resonance TCI probes. Data processing and analysis were carried out in Topspin (Bruker, Karlsruhe) and Sparky (Goddard & Kneller, University of California, San Francisco) respectively. ^{15}N fast HSQC experiments [66] were used to measure weighted chemical shift perturbations which were defined as $((\Delta^1H)^2)^{0.5}+((\Delta^{15}N / 5)^2)^{0.5}$ [ppm] [67]. In the case of shifted or doubled peaks, standard triple resonance experiments (HNCACB, CBCA(CO)NH and HNCA) were used to unambiguously assign all ^{15}N, ^{13}C backbone resonances. For a semi-quantitative assessment of exchange broadening, the apparent peak attenuation was plotted as the peak height difference between perturbed and unperturbed species. No attempt was made to correct for potential changes in the overall correlation times.

Crystallography

Lys6 triUb and tetraUb was crystallised at concentrations between 1-2 mg/mL in 50 mM Tris pH 7.4. Initial screening using sitting drop vapour diffusion resulted in several hits in conditions containing divalent cations. Optimisation of a condition containing 20% (v/v) PEG3350 and 0.2 M zinc acetate resulted in small cubic crystals. Prior to flash-cooling in liquid nitrogen, crystals were soaked briefly in mother liquor containing 15% (v/v) glycerol.

Diffraction data were collected at a wavelength of 0.979192 Å at the European Synchrotron Radiation Facility (ESRF, Grenoble) beamlines ID23, and ID14-4. The small crystals suffered from serious radiation damage, which limited data quality despite the high symmetry. The structure was determined using molecular replacement with the Met1-linked diUb structure (pdb-id 2w9n[29]). Simulated annealing in Phenix[68] to remove model bias, and subsequent rounds of manual model building and refinement in Coot[69] and Phenix resulted in final statistics shown in Table 1.

Calculating potential number of polyUb species

We found that the number of unique species of *n* Ub molecules in a chain linked via two branch points followed Catalan numbers[31] (1, 2, 5, 14, 42 for *n* from 1 to 5). A generalised formula for *n* Ub molecules linked via *k* linkages is eq. 1:

$$(kn)\,!/\,(n!\,(n\,(k-1)+1)\,!) \quad (1)$$

which we found empirically to give correct solutions for short polyUb chains.

Supplementary Material

Refer to Web version on PubMed Central for supplementary material.

Acknowledgements

We would like to thank David Yin-wei Lin and Jue Chen (Purdue University, West Lafayette, Indiana, USA) for kindly providing the NleL plasmid, and Trevor Rutherford and members of the Komander lab for helpful discussions. Tycho Mevissen, David Tourigny and Tobias Wauer are acknowledged for insights into combinatorial mathematics. Crystallographic data were collected at the European Synchrotron Radiation Facility (ESRF) at beam lines ID23-1, ID29 and ID14-4. This work was supported by the Medical Research Council [U105192732] and the EMBO Young Investigator Programme.

References

1. Hershko A, Ciechanover A. The ubiquitin system. Annu Rev Biochem. 1998; 67:425–479. [PubMed: 9759494]
2. Chen ZJ, Sun LJ. Nonproteolytic functions of ubiquitin in cell signaling. Mol Cell. 2009; 33:275–286. [PubMed: 19217402]
3. Al-Hakim A, et al. The ubiquitous role of ubiquitin in the DNA damage response. DNA Repair. 2010; 9:1229–1240. [PubMed: 21056014]
4. Acconcia F, Sigismund S, Polo S. Ubiquitin in trafficking: the network at work. Exp Cell Res. 2009; 315:1610–1618. [PubMed: 19007773]
5. Komander D, Rape M. The ubiquitin code. Annu Rev Biochem. 2012; 81:203–229. [PubMed: 22524316]
6. Kulathu Y, Komander D. Atypical ubiquitylation - the unexplored world of polyubiquitin beyond Lys48 and Lys63 linkages. Nat Rev Mol Cell Biol. 2012; 13:508–523. [PubMed: 22820888]
7. Behrends C, Harper JW. Constructing and decoding unconventional ubiquitin chains. Nat Struct Mol Biol. 2011; 18:520–528. [PubMed: 21540891]
8. Wickliffe KE, Williamson A, Meyer H-J, Kelly A, Rape M. K11-linked ubiquitin chains as novel regulators of cell division. Trends Cell Biol. 2011; 21:656–663. [PubMed: 21978762]
9. Chau V, et al. A multiubiquitin chain is confined to specific lysine in a targeted short-lived protein. Science. 1989; 243:1576–1583. [PubMed: 2538923]

10. Iwai K. Linear polyubiquitin chains: a new modifier involved in NFκB activation and chronic inflammation, including dermatitis. Cell Cycle. 2011; 10:3095–3104. [PubMed: 21900745]
11. Xu P, et al. Quantitative proteomics reveals the function of unconventional ubiquitin chains in proteasomal degradation. Cell. 2009; 137:133–145. [PubMed: 19345192]
12. Dammer EB, et al. Polyubiquitin linkage profiles in three models of proteolytic stress suggest the etiology of Alzheimer disease. J Biol Chem. 2011; 286:10457–10465. [PubMed: 21278249]
13. Kim W, et al. Systematic and quantitative assessment of the ubiquitin-modified proteome. Mol Cell. 2011; 44:325–340. [PubMed: 21906983]
14. Wagner SA, et al. A proteome-wide, quantitative survey of in vivo ubiquitylation sites reveals widespread regulatory roles. Molecular & Cellular Proteomics. 2011; 10 M111.013284.
15. Morris JR, Solomon E. BRCA1 : BARD1 induces the formation of conjugated ubiquitin structures, dependent on K6 of ubiquitin, in cells during DNA replication and repair. Hum Mol Genet. 2004; 13:807–817. [PubMed: 14976165]
16. Nishikawa H, et al. Mass spectrometric and mutational analyses reveal Lys-6-linked polyubiquitin chains catalyzed by BRCA1-BARD1 ubiquitin ligase. J Biol Chem. 2004; 279:3916–3924. [PubMed: 14638690]
17. Wu-Baer F, Lagrazon K, Yuan W, Baer R. The BRCA1/BARD1 heterodimer assembles polyubiquitin chains through an unconventional linkage involving lysine residue K6 of ubiquitin. J Biol Chem. 2003; 278:34743–34746. [PubMed: 12890688]
18. Wu W, et al. BRCA1 ubiquitinates RPB8 in response to DNA damage. Cancer Res. 2007; 67:951–958. [PubMed: 17283126]
19. Sato K, et al. Nucleophosmin/B23 is a candidate substrate for the BRCA1-BARD1 ubiquitin ligase. J Biol Chem. 2004; 279:30919–30922. [PubMed: 15184379]
20. Yu X, Fu S, Lai M, Baer R, Chen J. BRCA1 ubiquitinates its phosphorylation-dependent binding partner CtIP. Genes Dev. 2006; 20:1721–1726. [PubMed: 16818604]
21. Ben-Saadon R, Zaaroor D, Ziv T, Ciechanover A. The polycomb protein Ring1B generates self atypical mixed ubiquitin chains required for its in vitro histone H2A ligase activity. Mol Cell. 2006; 24:701–711. [PubMed: 17157253]
22. Oualid FE, et al. Chemical synthesis of ubiquitin, ubiquitin-based probes, and diubiquitin. Angew Chem Int Ed Engl. 2010; 49:10149–10153. [PubMed: 21117055]
23. Virdee S, Ye Y, Nguyen DP, Komander D, Chin JW. Engineered diubiquitin synthesis reveals Lys29-isopeptide specificity of an OTU deubiquitinase. Nat Chem Biol. 2010; 6:750–757. [PubMed: 20802491]
24. Husnjak K, Dikic I. Ubiquitin-binding proteins: decoders of ubiquitin-mediated cellular functions. Annu Rev Biochem. 2012; 81:291–322. [PubMed: 22482907]
25. Komander D, Clague MJ, Urbé S. Breaking the chains: structure and function of the deubiquitinases. Nat Rev Mol Cell Biol. 2009; 10:550–563. [PubMed: 19626045]
26. Reyes-Turcu FE, Ventii KH, Wilkinson KD. Regulation and cellular roles of ubiquitin-specific deubiquitinating enzymes. Annu Rev Biochem. 2009; 78:363–397. [PubMed: 19489724]
27. Lin DY-W, Diao J, Zhou D, Chen J. Biochemical and Structural Studies of a HECT-like Ubiquitin Ligase from Escherichia coli O157:H7. J Biol Chem. 2011; 286:441–449. [PubMed: 20980253]
28. Piscatelli H, et al. The EHEC Type III Effector NleL Is an E3 Ubiquitin Ligase That Modulates Pedestal Formation. PLoS ONE. 2011; 6:e19331. [PubMed: 21541301]
29. Komander D, et al. Molecular discrimination of structurally equivalent Lys 63-linked and linear polyubiquitin chains. EMBO Rep. 2009; 10:466–473. [PubMed: 19373254]
30. Dammer E, Peng J. At the crossroads of ubiquitin signaling and mass spectrometry. Expert Rev Proteomics. 2010; 7:643–645. [PubMed: 20973637]
31. Grimaldi, R. Fibonacci and Catalan Numbers. Wiley; 2012.
32. Bremm A, Freund SMV, Komander D. Lys11-linked ubiquitin chains adopt compact conformations and are preferentially hydrolyzed by the deubiquitinase Cezanne. Nat Struct Mol Biol. 2010; 17:939–947. [PubMed: 20622874]
33. Licchesi JDF, et al. An ankyrin-repeat ubiquitin-binding domain determines TRABID's specificity for atypical ubiquitin chains. Nat Struct Mol Biol. 2012; 19:62–71. [PubMed: 22157957]

34. Wang T, et al. Evidence for bidentate substrate binding as the basis for the K48 linkage specificity of otubain 1. J Mol Biol. 2009; 386:1011–1023. [PubMed: 19211026]
35. Akutsu M, Ye Y, Virdee S, Chin JW, Komander D. Molecular basis for ubiquitin and ISG15 cross-reactivity in viral ovarian tumor domains. Proceedings of the National Academy of Sciences. 2011; 108:2228–2233.
36. Ye Y, et al. Polyubiquitin binding and cross-reactivity in the USP domain deubiquitinase USP21. EMBO Rep. 2011; 12:350–357. [PubMed: 21399617]
37. Bang D, et al. Dissecting the energetics of protein alpha-helix C-cap termination through chemical protein synthesis. Nat Chem Biol. 2006; 2:139–143. [PubMed: 16446709]
38. Varadan R, et al. Solution conformation of Lys63-linked di-ubiquitin chain provides clues to functional diversity of polyubiquitin signaling. J Biol Chem. 2004; 279:7055–7063. [PubMed: 14645257]
39. Tenno T, et al. Structural basis for distinct roles of Lys63- and Lys48-linked polyubiquitin chains. Genes Cells. 2004; 9:865–875. [PubMed: 15461659]
40. Varadan R, Walker O, Pickart C, Fushman D. Structural properties of polyubiquitin chains in solution. J Mol Biol. 2002; 324:637–647. [PubMed: 12460567]
41. Reyes-Turcu FE, et al. The ubiquitin binding domain ZnF UBP recognizes the C-terminal diglycine motif of unanchored ubiquitin. Cell. 2006; 124:1197–1208. [PubMed: 16564012]
42. Lange OF, et al. Recognition dynamics up to microseconds revealed from an RDC-derived ubiquitin ensemble in solution. Science. 2008; 320:1471–1475. [PubMed: 18556554]
43. Fenwick RB, et al. Weak long-range correlated motions in a surface patch of ubiquitin involved in molecular recognition. J Am Chem Soc. 2011; 133:10336–10339. [PubMed: 21634390]
44. Prag G, et al. Mechanism of ubiquitin recognition by the CUE domain of Vps9p. Cell. 2003; 113:609–620. [PubMed: 12787502]
45. Dou H, Buetow L, Sibbet GJ, Cameron K, Huang DT. BIRC7-E2 ubiquitin conjugate structure reveals the mechanism of ubiquitin transfer by a RING dimer. Nat Struct Mol Biol. 2012; 19:876–883. [PubMed: 22902369]
46. Plechanovova A, Jaffray EG, Tatham MH, Naismith JH, Hay RT. Structure of a RING E3 ligase and ubiquitin-loaded E2 primed for catalysis. Nature. 2012; 489:115–120. [PubMed: 22842904]
47. Matsumoto ML, et al. K11-linked polyubiquitination in cell cycle control revealed by a K11 linkage-specific antibody. Mol Cell. 2010; 39:477–484. [PubMed: 20655260]
48. Kim HC, Steffen AM, Oldham ML, Chen J, Huibregtse JM. Structure and function of a HECT domain ubiquitin-binding site. EMBO Rep. 2011; 12:334–341. [PubMed: 21399621]
49. Maspero E, et al. Structure of the HECT:ubiquitin complex and its role in ubiquitin chain elongation. EMBO Rep. 2011; 12:342–349. [PubMed: 21399620]
50. Kamadurai HB, et al. Insights into Ubiquitin Transfer Cascades from a Structure of a UbcH5B∼Ubiquitin-HECTNEDD4L Complex. Mol Cell. 2009; 36:1095–1102. [PubMed: 20064473]
51. Perrett CA, Lin DY-W, Zhou D. Interactions of bacterial proteins with host eukaryotic ubiquitin pathways. Front. Microbio. 2011; 2:143.
52. Randow F, Lehner PJ. Viral avoidance and exploitation of the ubiquitin system. Nat Cell Biol. 2009; 11:527–534. [PubMed: 19404332]
53. Kim HT, et al. Certain pairs of ubiquitin-conjugating enzymes (E2s) and ubiquitin-protein ligases (E3s) synthesize nondegradable forked ubiquitin chains containing all possible isopeptide linkages. J Biol Chem. 2007; 282:17375–17386. [PubMed: 17426036]
54. Kim HT, Kim KP, Uchiki T, Gygi SP, Goldberg AL. S5a promotes protein degradation by blocking synthesis of nondegradable forked ubiquitin chains. EMBO J. 2009; 28:1867–1877. [PubMed: 19387488]
55. Sloper-Mould KE, Jemc JC, Pickart CM, Hicke L. Distinct functional surface regions on ubiquitin. J Biol Chem. 2001; 276:30483–30489. [PubMed: 11399765]
56. Messick TE, et al. Structural basis for ubiquitin recognition by the otu1 ovarian tumor domain protein. J Biol Chem. 2008; 283:11038–11049. [PubMed: 18270205]

57. Ye Y, Scheel H, Hofmann K, Komander D. Dissection of USP catalytic domains reveals five common insertion points. Mol Biosyst. 2009; 5:1797–1808. [PubMed: 19734957]
58. Vijay-Kumar S, Bugg CE, Cook WJ. Structure of ubiquitin refined at 1.8 A resolution. J Mol Biol. 1987; 194:531–544. [PubMed: 3041007]

Methods References

59. Trempe J-F, et al. Mechanism of Lys48-linked polyubiquitin chain recognition by the Mud1 UBA domain. EMBO J. 2005; 24:3178–3189. [PubMed: 16138082]
60. Komander D, et al. The structure of the CYLD USP domain explains its specificity for Lys63-linked polyubiquitin and reveals a B box module. Mol Cell. 2008; 29:451–464. [PubMed: 18313383]
61. Edelmann MJ, et al. Structural basis and specificity of human otubain 1-mediated deubiquitination. Biochem J. 2009; 418:379–390. [PubMed: 18954305]
62. Hu M, et al. Crystal structure of a UBP-family deubiquitinating enzyme in isolation and in complex with ubiquitin aldehyde. Cell. 2002; 111:1041–1054. [PubMed: 12507430]
63. Berrow NS, et al. A versatile ligation-independent cloning method suitable for high-throughput expression screening applications. Nucleic Acids Res. 2007; 35:e45. [PubMed: 17317681]
64. Pickart CM, Raasi S. Controlled synthesis of polyubiquitin chains. Meth Enzymol. 2005; 399:21–36. [PubMed: 16338346]
65. Raasi S, Pickart CM. Ubiquitin chain synthesis. Methods Mol Biol. 2005; 301:47–55. [PubMed: 15917625]
66. Mori S, Abeygunawardana C, Johnson MO, van Zijl PC. Improved sensitivity of HSQC spectra of exchanging protons at short interscan delays using a new fast HSQC (FHSQC) detection scheme that avoids water saturation. J Magn Reson B. 1995; 108:94–98. [PubMed: 7627436]
67. Hajduk PJ, et al. NMR-based discovery of lead inhibitors that block DNA binding of the human papillomavirus E2 protein. J. Med. Chem. 1997; 40:3144–3150. [PubMed: 9379433]
68. Adams PD, et al. The Phenix software for automated determination of macromolecular structures. Methods. 2011; 55:94–106. [PubMed: 21821126]
69. Emsley P, Lohkamp B, Scott WG, Cowtan K. Features and development of Coot. Acta Crystallogr D Biol Crystallogr. 2010; 66:486–501. [PubMed: 20383002]

Europe PMC Funders Author Manuscripts

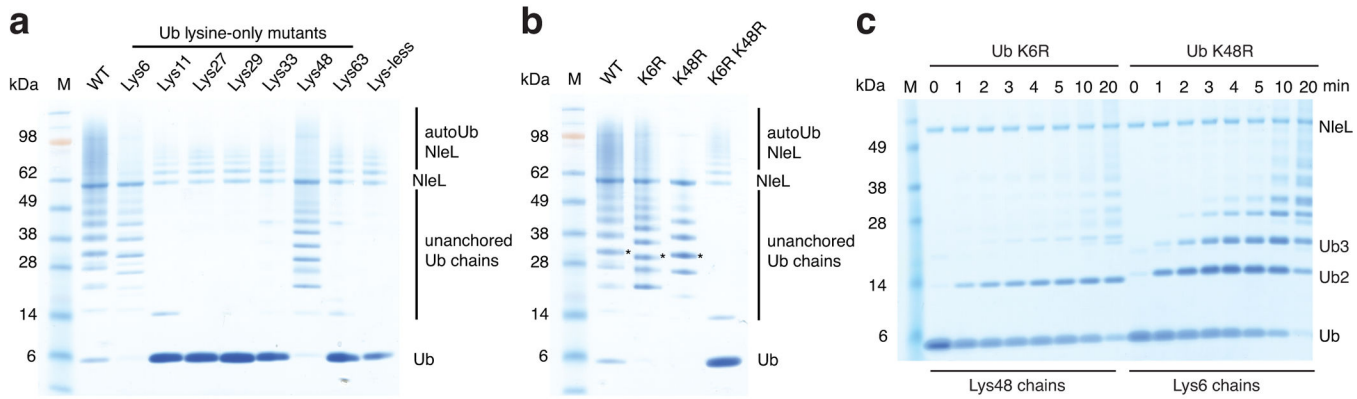

Figure 1. NleL-mediated Ub chain assembly

(a) NleL was used in Ub chain assembly reactions with E1, UBE2L3/UbcH7, and Ub mutants as indicated (see **Methods**). M, marker; WT, wild type Ub; Ub-lysine only, Ub mutants with Arg mutations in six out of seven Lys residues; Lys-less, Ub harbouring Arg mutations at all Lys residues. **(b)** A comparison of assembled unanchored Ub chains from WT Ub, Ub K6R and Ub K48R. A Ub K6R K48R double mutant is unable to assemble similar unanchored Ub products. Asterisks (*) indicate pentaUb species. **(c)** Time-course analysis of the NleL assembly reaction as in **a** with Ub K6R or Ub K48R.

Europe PMC Funders Author Manuscripts

Europe PMC Funders Author Manuscripts

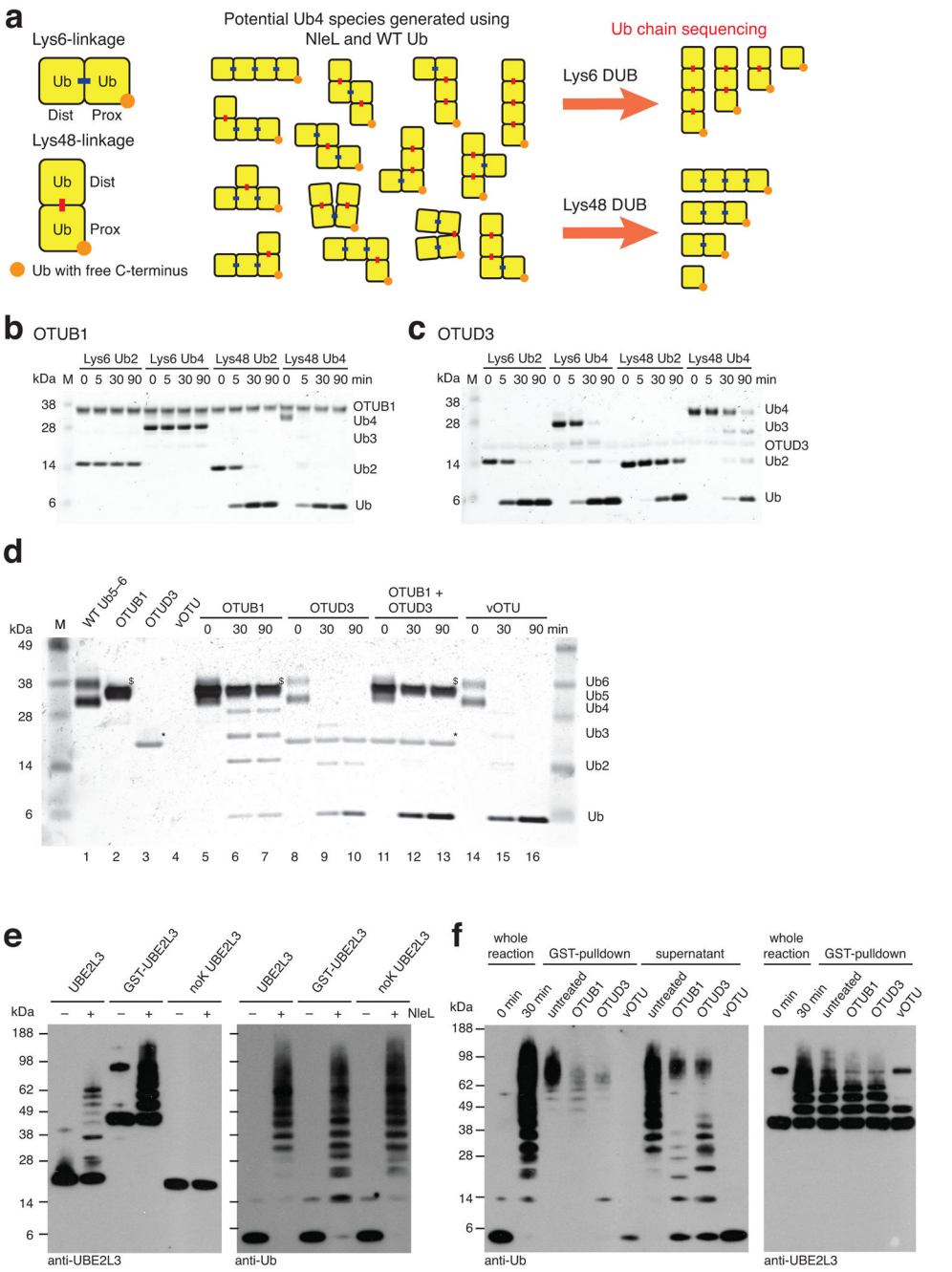

Figure 2. Ub chain sequencing using linkage-specific DUBs

(a) Schematic illustrating potential tetramer complexity in NleL assembled WT Ub products, and the concept of Ub chain restriction mapping. Ub (yellow square) can be linked either *via* Lys6 (blue line; horizontal) or Lys48 (red line; vertical), leading to 14 distinct species. An orange dot indicates the free C-terminus of Ub (proximal moiety). Linkage-specific DUBs can be used as 'Ub chain restriction enzymes' to reveal building blocks within heterotypic Ub chains. **(b, c)** Specificity profile of OTUB1 at 4.7 μM **(b)** and OTUD3 at 5.5 μM **(c)** against Lys6 and Lys48 diUb and tetraUb. Hydrolysis of polyUb is followed

during the indicated time-course, and resolved on a silver-stained SDS-PAGE gel. **(d)** Purified penta / hexaUb assembled from WT Ub (lane 1) is cleaved with 4.7 μM OTUB1, 5.5 μM OTUD3, 6.1 nM vOTU or combinations thereof. *, OTUD3 protein; $, OTUB1 protein. **(e)** NleL mediated ubiquitination of UBE2L3 variants as in Fig. 1a, detected by Western blotting with anti-UBE2L3 (left) and anti-Ub antibodies (right). noK UBE2L3, UBE2L3 mutant with 18 Lys residues changed to Arg. **(f)** DUB assays performed for 1 h as in **d**, on polyubiquitinated GST-tagged UBE2L3 from **e**, analysed by Western blotting as in **e**. Whole reaction, samples before GST-pulldown; supernatant, reaction after GST-pulldown containing free NleL assembled Ub chains. Lys6 polyUb detection is less efficient compared to Lys48 polyUb, compare **f** to **d**. Prox, proximal; Dist, distal; M, marker; WT, wild type.

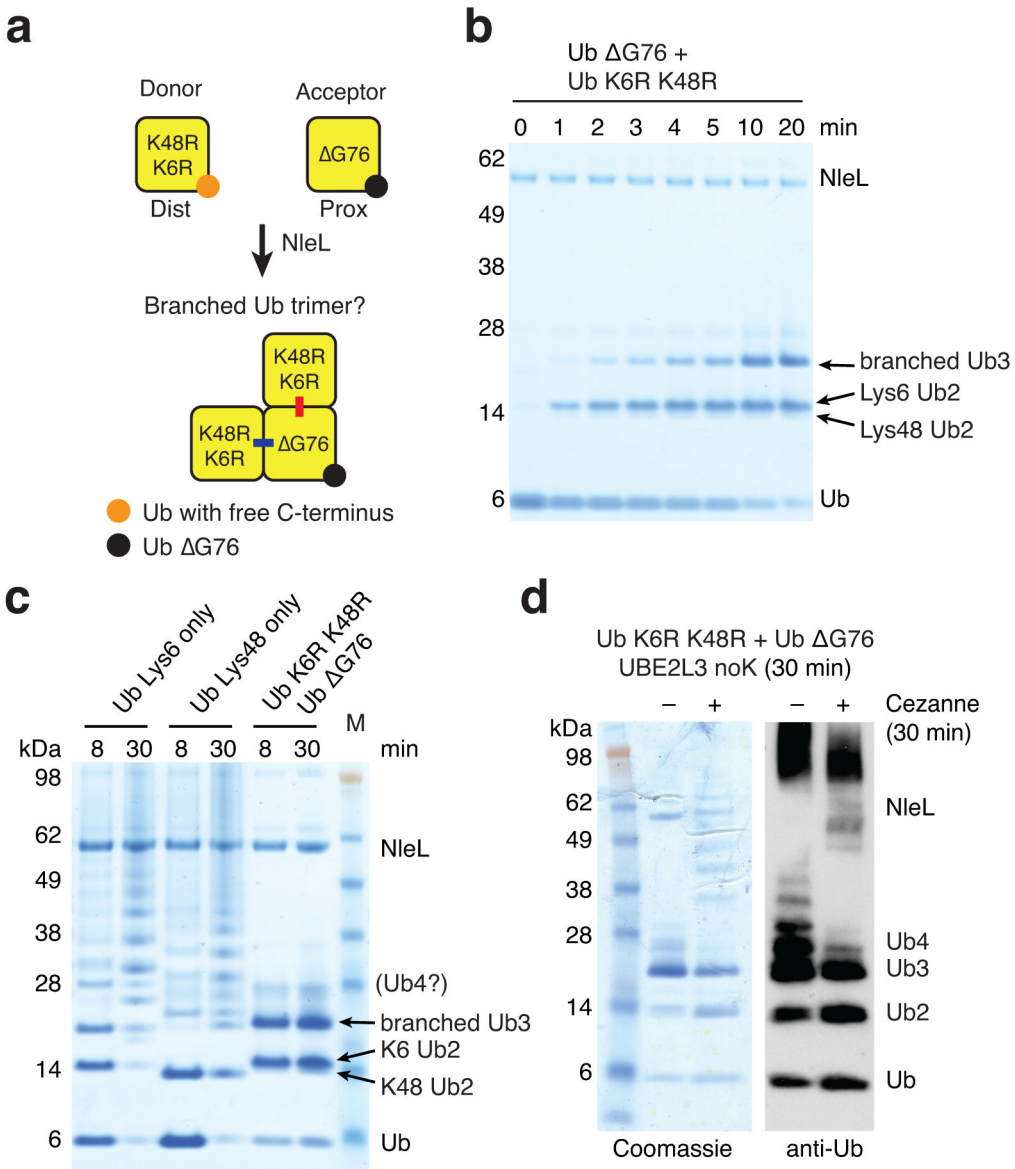

Figure 3. NleL assembles branched Ub chains

(a) Schematic depicting the assembly of a branched triUb harbouring one Lys6- and one Lys48-linkage. **(b)** Time-course analysis of NleL assembly reaction (as in Fig. 1c) with a combination of 19 μM Ub ΔG76 (Acceptor) and 38 μM Ub K6R K48R (Donor). **(c)** NleL mediated assembly of Ub chains from Ub K6 only, Ub K48 only and a combination of Ub ΔG76 and Ub K6R K48R in a 1:2 molar ratio as in **b**. Resulting species are labelled. An emerging tetraUb band that also appears in **b** is labelled. M, marker. **(d)** DUB assay using the Lys11-linkage specific DUB Cezanne[32]. A 30 min reaction is performed with noK UBE2L3 (Fig. 2e) to exclude autoubiquitination of the E2, and subsequently treated with 2 μM Cezanne for 30 min, which selectively removes the tetraUb species.

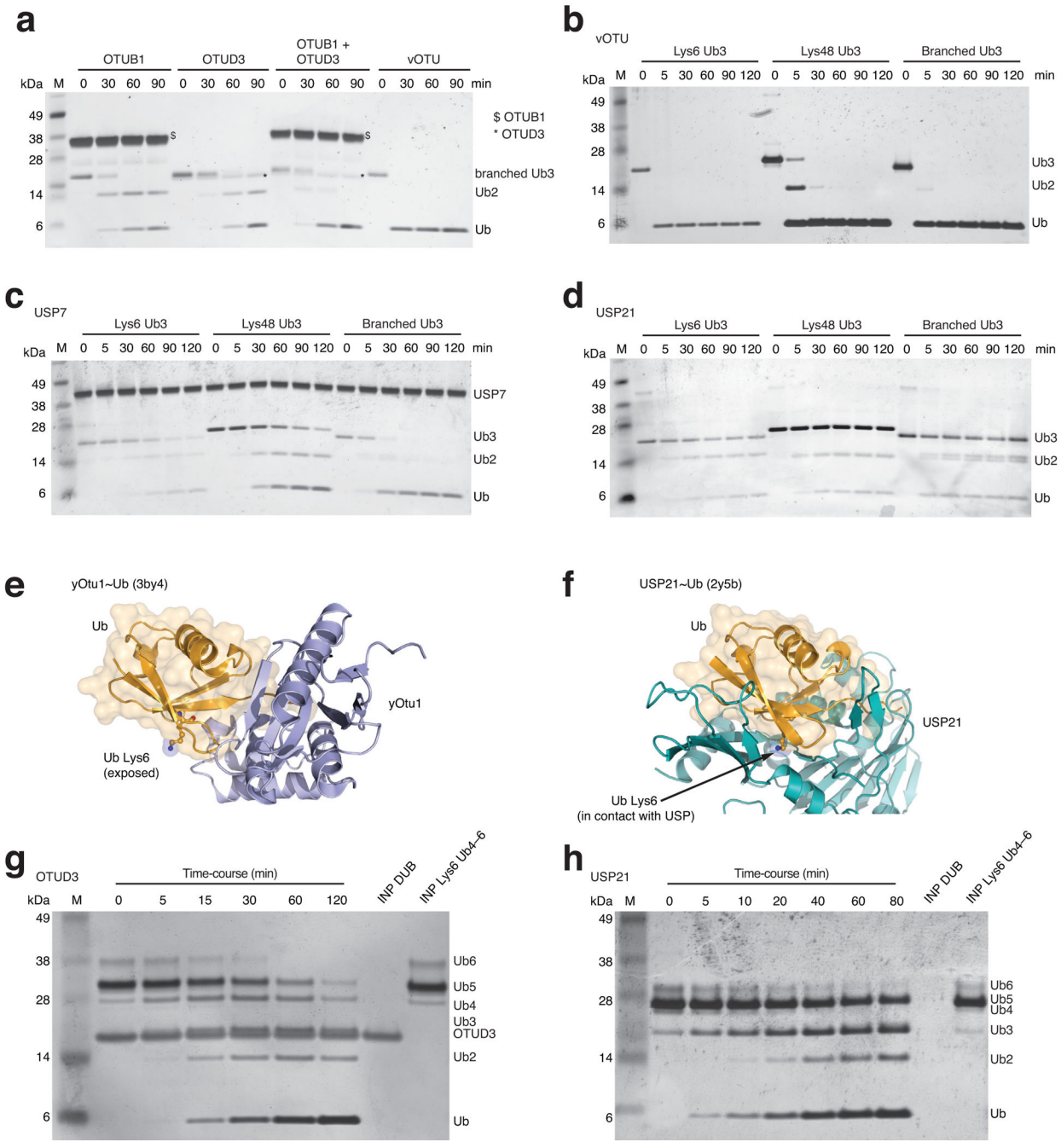

Figure 4. Hydrolysis of branched and Lys6-linked polyUb by DUBs

(a) Branched triUb was hydrolysed with 4.7 μM OTUB1, 5.5 μM OTUD3 or 6.1 nM vOTU. A silver-stained SDS-PAGE gel is shown. **(b-d)** Hydrolysis of homotypic Lys6 triUb, homotypic Lys48 triUb and branched triUb containing one Lys6- and one Lys48-linkage (see Fig. 3) by 6.1 nM vOTU **(b)**, 2.5 μM USP7 **(c)** and 60 nM USP21 **(d)**, performed as in **a**. All tested DUBs hydrolyse branched triUb similarly to homotypic Ub chains. **(e)** Structure of *S. cerevisiae* Otu1 (yOtu1, blue, pdb-id 3by4, [56]) covalently bound to Ub (orange). Ub Lys6 is shown in stick-representation, and is solvent exposed. **(f)** Structure of

USP21 (green) in complex with Ub (orange) (pdb-id 2y5b,[36]). Ub Lys6 (indicated with an arrow) is at the interface with the USP core, interacting with Glu427, which is highly conserved amongst USP DUBs[57]. Ub is shown in the same orientation as in **e**. **(g)** Time-course DUB assay of OTUD3 cleavage of Lys6 chains. DiUb is generated at each time point, indicating that OTUD3 cleaves any linkage in the chain (*endo*-activity). **(h)** Time-course DUB assay of USP21 cleavage of Lys6 chains. DiUb is generated only at later time point, indicating that USP21 hydrolyses Lys6 polymers from the distal end with *exo*-activity, consistent with the structure. M, marker; INP, input.

Europe PMC Funders Author Manuscripts

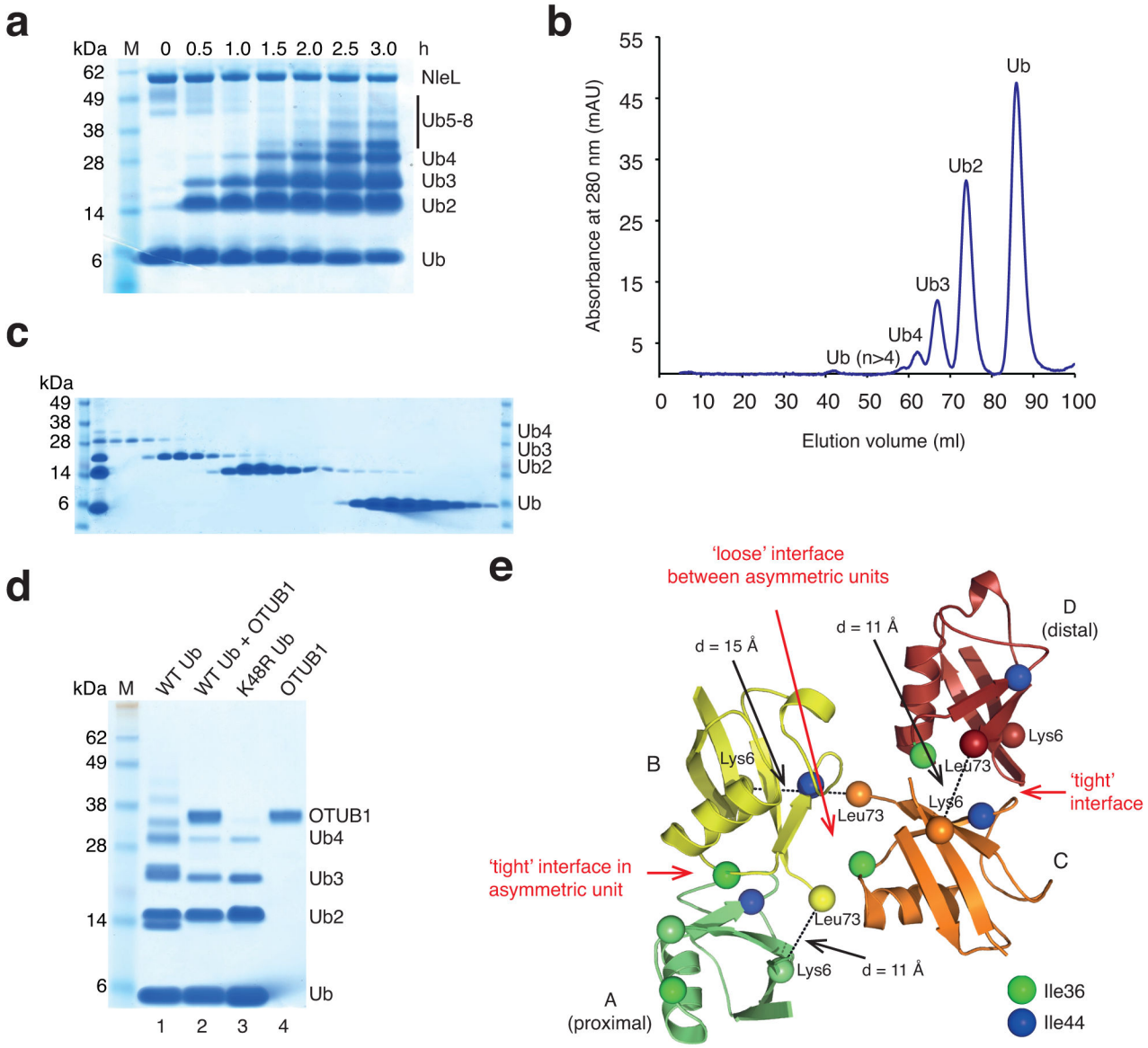

Figure 5. Large-scale assembly and crystal structures of Lys6 polyUb

(a) Time-course analysis of a large-scale assembly reaction of Lys6 polyUb by NleL using 25 mg Ub K48R as input material, as described in **Methods**. **(b)** Chromatogram of purification of Lys6 polyUb species by size-exclusion chromatography (SEC). **(c)** Fractions corresponding to individual peaks from SEC purification in **b** are resolved by SDS-PAGE. **(d)** Comparison of the assembly reactions performed by NleL using WT Ub (lane 1), Ub K48R (lane 2) and WT Ub subsequently treated using 5.1 μM OTUB1 for 3 h (lane 3). Large-scale reactions can be treated with OTUB1 overnight. M, marker; WT, wild type. **(e)** Packing of Lys6 polyUb crystals, two neighbouring asymmetric units are shown, in which Ub molecules interact via a 'tight' interface (witin asymmetric unit) or via a 'loose' interface between asymmetric units. Green and blue spheres indicate the Cα positions of Ile36 and Ile44, respectively. Distances indicated by a black dotted line refer to Cα atoms of Leu73 and Lys6 in neighbouring moieties.

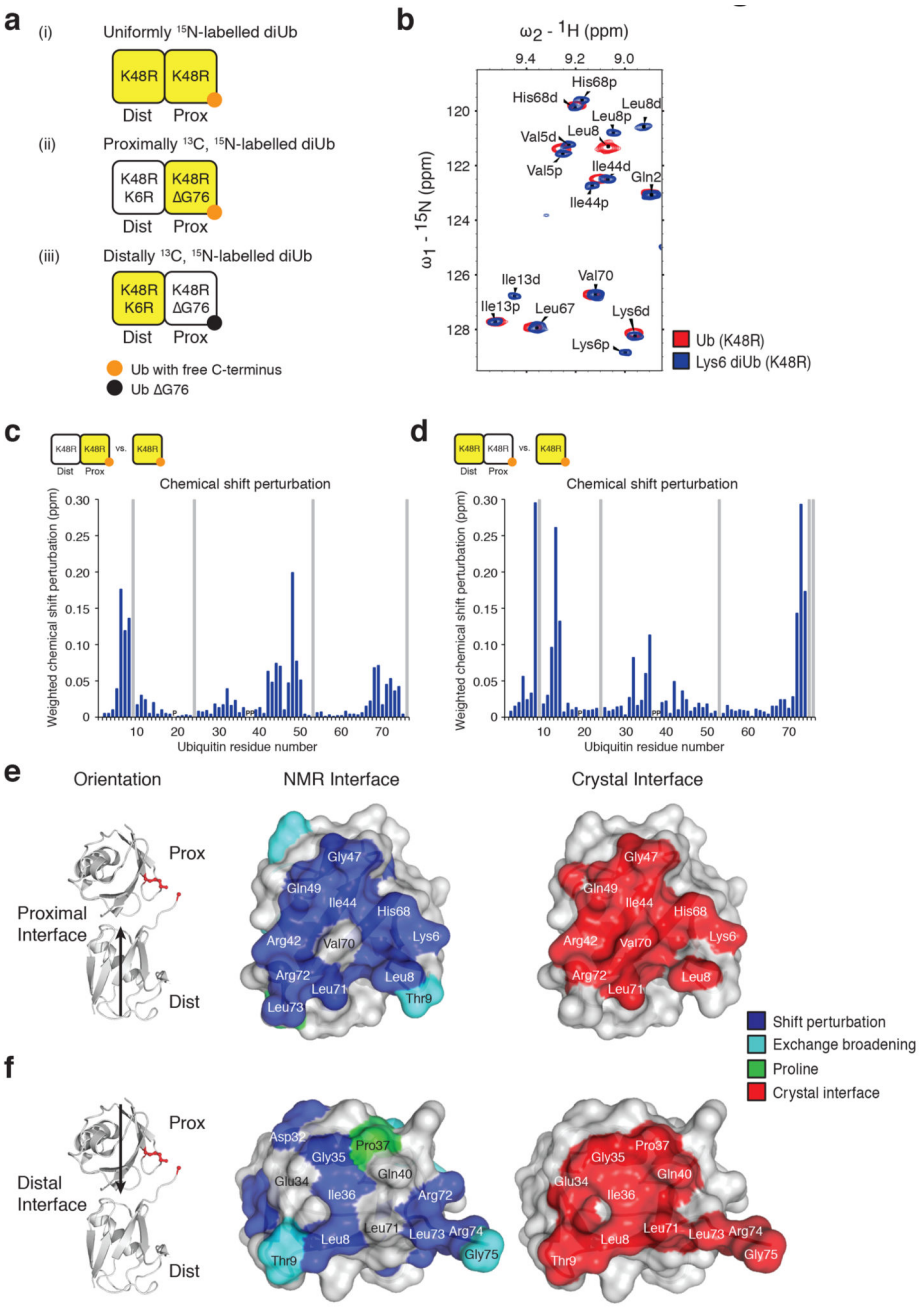

Figure 6. Solution studies of Lys6 diUb

(a) Schematic of Lys6 diUb species generated for NMR analysis. Ub moieties coloured in yellow are isotopically labelled. Mutations made to generate these Lys6 diUb species are indicated. **(b)** Selected region of ^{1}H, ^{15}N-HSQC spectra showing the ^{15}N-labelled Lys6 diUb (blue) (i) overlaid onto Ub K48R (red). For full spectra see Supplementary Fig. 6a. Reassigned spectra from proximally (ii) and distally (iii) labelled Lys6 diUb (Supplementary Fig. 6b, c) allow unambiguous assignment of distal (d) and proximal (p) resonances in the uniformly ^{15}N-labelled spectrum. **(c, d)** Weighted chemical shift perturbation (CSP) map

from **b** for the proximal **(c)** and distal **(d)** molecule (see also Supplementary Fig. 5a). Grey bars, exchange broadened residues; (P), prolines. **(e, f)** *Left*, 'tight' interface of Lys6 polyUb indicating **(e)** proximal and **(f)** distal interfaces. *Middle*, significant CSPs were mapped onto the surface of Ub. Blue, CSPs >0.035 ppm; cyan, exchange broadened residues; green, prolines. *Right*, crystallographic interface according to PISA analysis (http://www.ebi.ac.uk/msd-srv/prot_int/pistart.html) mapped onto the surface of Ub in red. Prox, proximal; Dist, distal.

Europe PMC Funders Author Manuscripts

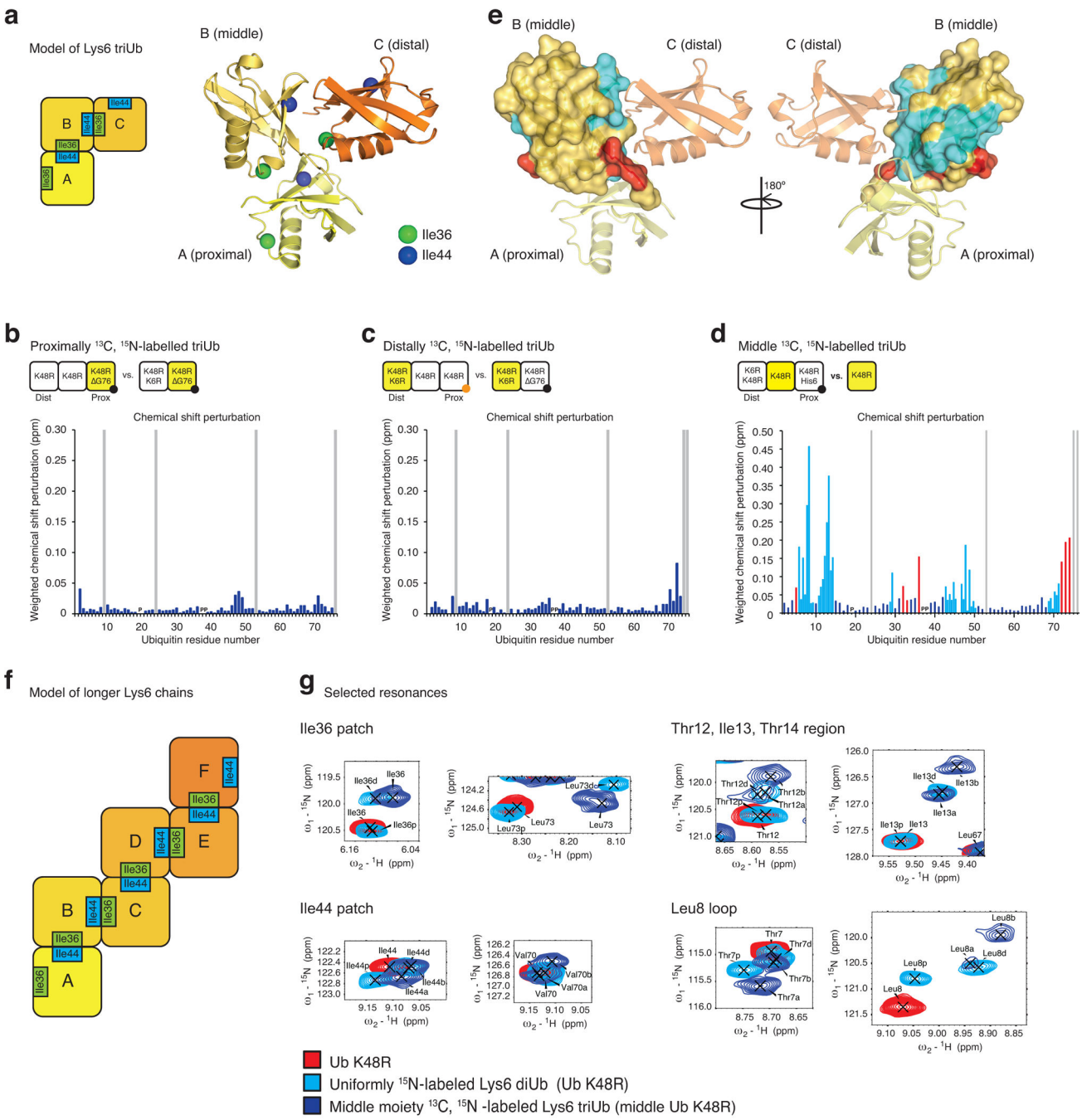

Figure 7. Solution studies of Lys6 triUb by NMR spectroscopy

(a) Schematic and molecular model of Lys6 triUb where the 'tight' Ile44-Ile36 interface is propagated (compare Fig. 5e). The Cα atoms of Ile36 (green) and Ile44 (blue) are indicated as spheres. **(b)** NMR analysis of proximally labelled Lys6 triUb. *Top*, a schematic of the experiments showing the compared species. Ub moieties coloured in yellow are isotopically labelled. Weighted CSP map for Lys6 triUb with respect to Lys6 diUb. Grey bars, exchange-broadened residues; (P), prolines. For full spectra see Supplementary Fig. 7a. (c) Analysis as in **b** for distally labelled Lys6 triUb compared to monoUb K48R. For full

Europe PMC Funders Author Manuscripts

spectra see Supplementary Fig. 7b. (d) Analysis as in **b** for a middle labelled Lys6 triUb. The CSP map indicates resonances that are shifted compared to monoUb K48R. Resonances that are shifted and overlay with the distal resonance position in uniformly labelled diUb (Fig. 6b) are indicated in red, and split resonances in cyan. For full spectra see Supplementary Fig. 8. (e) Mapping of perturbed residues onto the surface of Ub shown in two orientations. **(f)** NMR supports a model for longer Lys6 polyUb in which the asymmetric Ile36-Ile44 patch interactions are propagated. **(g)** Selected resonances from the middle labelled triUb species. Each panel shows a residue in the $^{1}H,^{15}N$-HSQC spectra of middle labelled Lys6 triUb (blue) overlaid onto uniformly labelled Lys6 diUb (green, Fig. 6b) and monoUb K48R (red, Fig. 6b). In the diUb spectrum proximal (p) and distal (d) positions are indicated, whereas in the triUb spectrum split resonances are arbitrarily assigned a and b. See Supplementary Fig. 4 for additional resonances. Prox, proximal; Dist, distal.

Europe PMC Funders Author Manuscripts

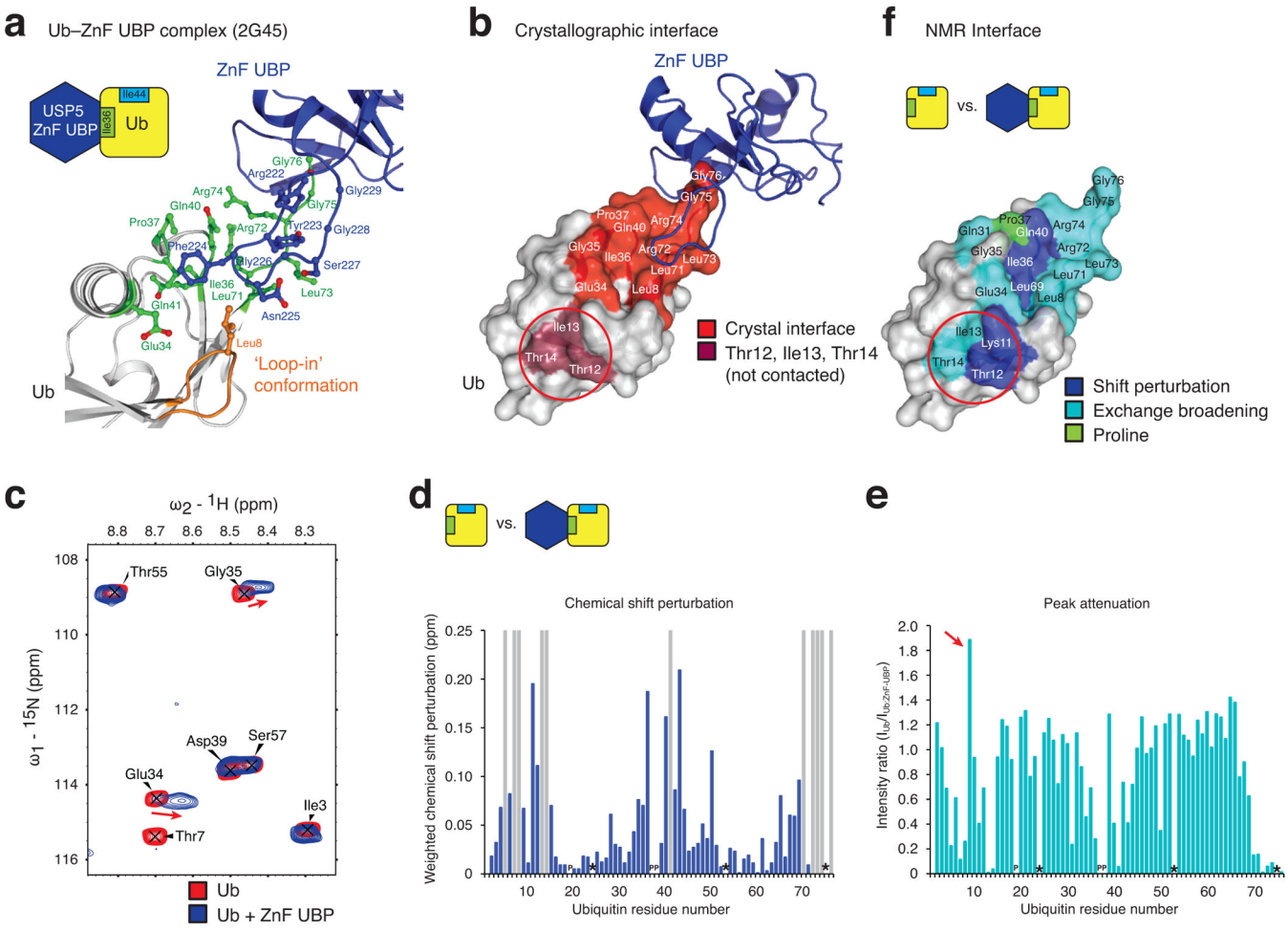

Figure 8. Ile36 binding causes structural rearrangements in Ub

(a) Schematic representation and close-up of the ZnF UBP interaction with Ub. **(b)** Interacting residues according to PISA analysis are coloured on the Ub surface (red), and residues 12-14 on the β2-strand of Ub (purple, circled) are not involved in the interaction. **(c)** Selected region of ^{1}H, ^{15}N-HSQC spectra for a 1:1 molar complex of Ub with ZnF UBP (blue) overlaid onto Ub (red). Ub was ^{13}C,^{15}N-labelled and ZnF UBP was unlabelled. Resonances experience chemical shifts (Glu34), exchange broadening (Thr7) or are unperturbed (Ile3). For full spectra see Supplementary Fig. 9. **(d)** *Top*, schematic of the experiment showing the compared species. Weighted CSP map derived from spectra in **c**. Grey bars, residues completely exchange broadened in the Ub–ZnF UBP complex; Asterisk (*), residues exchange broadened already in Ub; (P), prolines. See also Supplementary Fig. 4b. **(e)** Peak height attenuation map derived from spectra in **c** indicating the degree of exchange broadening upon complex formation. Asterisk (*), residues exchange broadened already in Ub; (P), prolines. Thr9 (red arrow) is exchange broadened in monoUb but reappears when Ub is in complex with ZnF UBP. See also Supplementary Fig. 4b. **(f)** Significant CSPs were mapped onto the surface of Ub. Blue, CSPs >0.09 ppm; cyan, exchange broadened residues (intensity ratio <0.5); green, prolines. Circled residues Thr12, Ile13, Thr14 are perturbed but not involved in the interface.

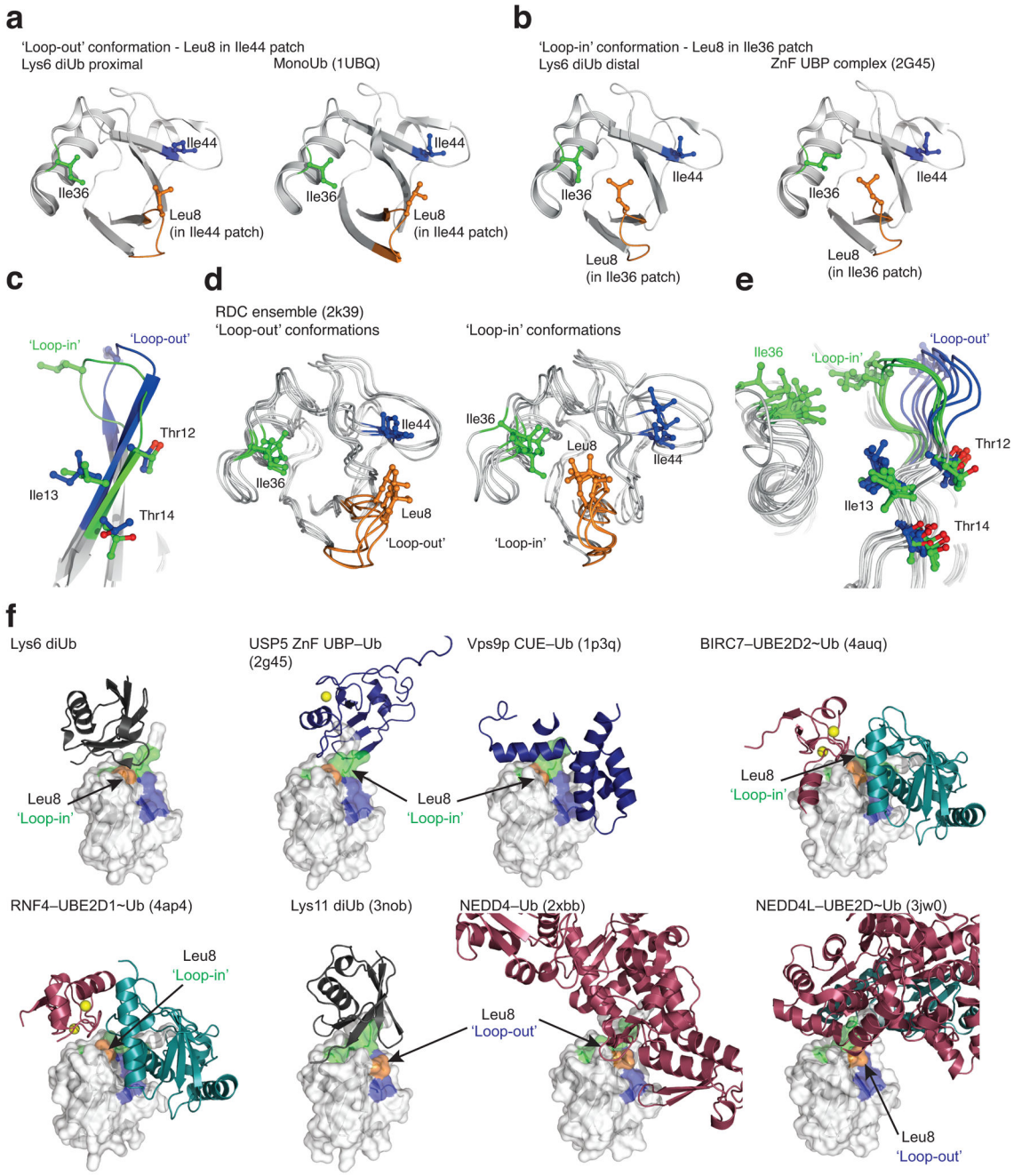

Figure 9. Ub 'loop-in' and 'loop-out' conformations

(a) Ub in the 'loop-out' conformation with Leu8 contributing to the Ile44 patch. *Left*, proximal Ub from Lys6 diUb. *Right*, monoUb (pdb-id 1ubq[58]). **(b)** Ub in the 'loop-in' conformation with Leu8 contributing to the Ile36 patch. *Left*, distal Ub from Lys6 diUb. *Right*, Ub bound to USP5 ZnF UBP (2g45[41]). **(c)** Comparison of Ub from **a** (blue) with Ub from **b** (green), showing the displacement of the β2-strand it the 'loop-in' conformation. **(d)** Both loop conformations are found in the RDC ensemble of Ub[42]. Four representative examples for each conformation are shown. Ile44 is in a more flexible region when Ub is in

the ‘loop-in’ conformation. **(e)** Overlay of the eight Ub conformations from **d**, showing residues Thr12, Ile13 and Thr14 on the β2-strand of Ub. The ‘loop-in’ conformation shifts the β2-strand outwards. (**f**) Ub is shown in surface representation (white) and in identical orientations with the Ile44 patch coloured in blue, the Ile36 patch in green and Leu8 in orange. The ubiquitin interacting protein is shown in cartoon representation. The position of the β1/β2-loop in the ‘loop-in’ or ‘loop-out’ conformation is indicated. Structures from top left to bottom right: Lys6 diUb (2xk5[23]), USP5 ZnF UBP (2g45[41]), Vps9p CUE domain (1p3q[44]), BIRC7 RING domain in complex with Ub-charged UBE2D2 (4auq[45]), RNF4 RING domain bound to Ub-charged UBE2D1 (4ap4[46]), Lys11 diUb (3nob[47]), Ub bound to the NEDD4 N-lobe (2xbb[49]), NEDD4L in complex with an UBE2D~Ub oxyester (3jw0[50]).

Table 1

Data collection and refinement statistics.

	Lys6 triUb
Data collection	
Space group	$P4_332$
Cell dimensions	
a, b, c (Å)	104.93, 104.93, 104.93
α,β,γ (°)	90, 90, 90
Resolution (Å)	74.20 – 2.90 (3.06-2.90) *
R_{merge}	0.127 (0.680)
$I / \sigma I$	7.4 (2.2)
Completeness (%)	97.2 (99.3)
Redundancy	4.5 (4.6)
Refinement	
Resolution (Å)	29.10 – 3.00
No. reflections	4112
R_{work} / R_{free}	0.230 / 0.287
No. atoms	
Protein	1000
Ligand/ion	5
B-factors	
Protein	70.3
Ligand/ion	99.3
R.m.s. deviations	
Bond lengths (Å)	0.006
Bond angles (°)	0.966

* Values in parentheses are for highest-resolution shell.